LAWRENCE
LIVERMORE
NATIONAL
LABORATORY

UCRL-PROC-203343

Implementation of Frictional Contact Conditions in Surface to Surface, Mortar Based Computational Frameworks

T. A. Laursen, B. Yang, M. A. Puso

April 2, 2004

European Congress on Compuational Methods in Applied Sciences and Engineering
Jyvaskyla, Finland
July 24, 2004 through July 28, 2004

This work was performed under the auspices of the U.S. Department of Energy by the University of California, Lawrence Livermore National Laboratory under Contract No. W-7405-Eng-48.

European Congress on Computational Methods in Applied Sciences and Engineering
ECCOMAS 2004
P. Neittaanmäki, T. Rossi, S. Korotov, E. Oñate, J. Périaux, and D. Knörzer (eds.)
Jyväskylä, 24–28 July 2004

IMPLEMENTATION OF FRICTIONAL CONTACT CONDITIONS IN SURFACE TO SURFACE, MORTAR BASED COMPUTATIONAL FRAMEWORKS

Tod A. Laursen[⋆], Bin Yang[⋆], and Michael A. Puso[†]

[⋆]Department of Civil and Environmental Engineering
Duke University, Box 90287, Durham, NC 27708, USA
e-mails: laursen@duke.edu, by5@duke.edu

[†] Lawrence Livermore National Laboratory
P.O. Box 808, Livermore, CA 94550, USA
e-mail: puso@llnl.gov

Key words: Contact, Friction, Mortar Methods, Finite Elements.

Abstract. *A number of recent works have established the* mortar technique *as an accurate and robust spatial discretization method for contact problems in computational solid mechanics. Since methods based on this idea rely on an integral, non-local representation of the contact operators, their formulation is somewhat more involved than is true for more traditional "point to surface" contact algorithms; in particular, the integral projections have nontrivial linearizations in the fully large deformation context. In this work, we concentrate on another aspect of formulations of this type—definition and implementation of frictional contact operators within the mortar contact framework. Issues associated with frame indifference of frictional tractions and kinematics are discussed, and a numerical demonstration of the technique is given.*

1 INTRODUCTION

Several authors in recent years (see [1, 3]) have demonstrated the utility of the mortar framework in including accurate and stable spatial discretizations of contact phenomena in finite element calculations. However, such algorithms have been robustly implemented only recently (see [4, 5]) in a true large deformation, large sliding context. Many of the challenges associated with the large sliding problem have to do with the linearization of the mortar projection operators. Since in large sliding these projection operators depend strongly on the position of one surface relative to the other, the operators must be differentiated to obtain a consistent tangent stiffness that will facilitate effective implicit finite element simulations. The considerable effort and expense associated with this linearization has been shown to lead to a highly robust contact algorithm, as the nonlocal characteristics of the mortar contact operators gives rise not only to enhanced spatial accuracy of the scheme, but also to considerable smoothing of many of the discontinuities which tend to plague Newton-Raphson treatments of contact.

In this work, we focus specifically on issues associated with the implementation of *friction* within the surface to surface contact framework. In particular, implementation of frictional conditions requires appropriate notions of relative velocity and rates of frictional tractions, in which frame indifference must be assured. We discuss the adaptation of frame indifferent formulations of frictional contact to the nonlocal surface to surface framework, and demonstrate the effectiveness of these formulations in a two dimensional application.

2 GENERAL PROBLEM DEFINITION

We consider a two body contact problem, with the bodies in question (indexed by (i)) assumed to contact sometime during the time interval $[0, T]$ of interest. We seek to find the motions $\boldsymbol{\varphi}^{(i)}$ of the two bodies (i), defined over their reference domains $\Omega^{(i)}$, for all times t in this interval. The virtual work principle for the two body contact problem in large deformations can be written at any time t by appealing to admissible variations $\overset{*}{\boldsymbol{\varphi}}{}^{(i)}$ via

$$
\begin{aligned}
G(\boldsymbol{\varphi}, \overset{*}{\boldsymbol{\varphi}}) &:= \sum_{i=1}^{2} G^{(i)}(\boldsymbol{\varphi}^{(i)}, \overset{*}{\boldsymbol{\varphi}}{}^{(i)}) \\
&= \sum_{i=1}^{2} \Bigg\{ \int_{\Omega^{(i)}} \left[\rho_0 \overset{*}{\boldsymbol{\varphi}}{}^{(i)} \cdot \boldsymbol{A}^{(i)} + Grad \overset{*}{\boldsymbol{\varphi}} : \boldsymbol{P}^{(i)} \right] d\Omega \\
&\qquad - \int_{\Omega^{(i)}} \overset{*}{\boldsymbol{\varphi}}{}^{(i)} \cdot \boldsymbol{F}^{(i)} d\Omega - \int_{\Gamma_\sigma^{(i)}} \overset{*}{\boldsymbol{\varphi}}{}^{(i)} \cdot \bar{\boldsymbol{T}}^{(i)} d\Gamma \Bigg\} \\
&\qquad - \sum_{i=1}^{2} \int_{\Gamma_c^{(i)}} \overset{*}{\boldsymbol{\varphi}}{}^{(i)} \cdot \boldsymbol{t}^{(i)} d\Gamma = 0 \\
&= G^{int,ext}(\boldsymbol{\varphi}, \overset{*}{\boldsymbol{\varphi}}) + G^{c}(\boldsymbol{\varphi}, \overset{*}{\boldsymbol{\varphi}}) = 0.
\end{aligned}
\tag{1}
$$

In (1), $G^{int,ext}(\boldsymbol{\varphi}, \overset{*}{\boldsymbol{\varphi}})$ is the sum of the virtual work arising from the internal and external forces, while the notation $G^c(\boldsymbol{\varphi}, \overset{*}{\boldsymbol{\varphi}})$ denotes the virtual work associated with the contact tractions. The notation $\boldsymbol{A}^{(i)}$ has been employed to denote the material acceleration field in body (i) (in the event that inertial effects are present), $\boldsymbol{F}^{(i)}$ denotes the body force in body (i), $\boldsymbol{P}^{(i)}$ denotes the Piola tractions, and $\bar{\boldsymbol{T}}^{(i)}$ denotes the prescribed (reference) tractions that may be prescribed over some portion $\Gamma_\sigma^{(i)}$ of each body's boundary, assumed to be nonintersecting with both the Dirichlet portion of the boundary of the body in question, and the subset $\Gamma_c^{(i)}$ of the body's surface where contact interaction may occur (with Piola tractions $\boldsymbol{t}^{(i)}$ acting over those portions of the boundary).

We proceed to discretize the contact interaction by writing the contact virtual work as

$$\begin{aligned} G^c(\boldsymbol{\varphi}, \overset{*}{\boldsymbol{\varphi}}) &= -\sum_{i=1}^{2} \int_{\Gamma_c^{(i)}} \overset{*}{\boldsymbol{\varphi}}^{(i)} \cdot \boldsymbol{t}^{(i)} d\Gamma \\ &= G^{cm}(\boldsymbol{\varphi}, \overset{*}{\boldsymbol{\varphi}}) \\ &= -\sum_{i=1}^{2} \int_{\gamma_c^{(i)}} \overset{*}{\boldsymbol{\varphi}}^{(i)} \cdot \boldsymbol{\lambda}^{(i)} d\gamma, \end{aligned} \tag{2}$$

where $G^{cm}(\boldsymbol{\varphi}, \overset{*}{\boldsymbol{\varphi}})$ will be used to denote the mortar element version of the contact virtual work. The notation $\gamma_c^{(i)}$ indicates the current configuration of $\Gamma_c^{(i)}$, so that the mortar multiplier $\boldsymbol{\lambda}^{(i)}$ is utilized to mean the Cauchy contact traction. Balance of linear momentum across the contact interface implies that (2) simplifies to:

$$G^{cm}(\boldsymbol{\varphi}, \overset{*}{\boldsymbol{\varphi}}) := -\int_{\gamma_c^{(1)}} \boldsymbol{\lambda}^{(1)} \cdot \left(\overset{*}{\boldsymbol{\varphi}}^{(1)} - \overset{*}{\boldsymbol{\varphi}}^{(2)} \right) d\gamma. \tag{3}$$

To draw the correspondence with the mortar literature, the slave surface $\gamma_c^{(1)}$ is referred to as the *nonmortar* surface, as it is the one where the Lagrange multipliers will be interpolated, while the master surface $\gamma_c^{(2)}$ is called the *mortar* surface.

2.1 Mortar Discretization of the Contact Integral

The overall structure of the mortar framework approach to contact is developed by writing expansions for the above contact surface fields in terms of finite element shape functions, and substituting the results into (3). The discretized multipliers, the deformation fields and their variations on the contact surface may be interpolated as

$$\boldsymbol{\lambda}^h(\boldsymbol{X}) = \sum_{A=1}^{n_s} N_A^{(1)} \left(\xi^{(1)}(\boldsymbol{X}) \right) \boldsymbol{\lambda}_A, \tag{4}$$

$$\boldsymbol{\varphi}^{(1)^h}(\boldsymbol{X}) = \sum_{D=1}^{n_s} N_D^{(1)} \left(\xi^{(1)}(\boldsymbol{X}) \right) \boldsymbol{\varphi}_D^{(1)}, \tag{5}$$

$$\boldsymbol{\varphi}^{(2)^h}(\bar{\boldsymbol{Y}}) = \sum_{E=1}^{n_m} N_E^{(2)}\left(\xi^{(2)}(\bar{\boldsymbol{Y}})\right)\boldsymbol{\varphi}_E^{(2)}, \tag{6}$$

$$\overset{*}{\boldsymbol{\varphi}}{}^{(1)^h}(\boldsymbol{X}) = \sum_{B=1}^{n_s} N_B^{(1)}\left(\xi^{(1)}(\boldsymbol{X})\right)\overset{*}{\boldsymbol{\varphi}}{}_B^{(1)}, \tag{7}$$

$$\overset{*}{\boldsymbol{\varphi}}{}^{(2)^h}(\bar{\boldsymbol{Y}}) = \sum_{C=1}^{n_m} N_C^{(2)}\left(\xi^{(2)}(\bar{\boldsymbol{Y}})\right)\overset{*}{\boldsymbol{\varphi}}{}_C^{(2)}, \tag{8}$$

where A, B and D are indices associated with slave (nonmortar) nodes, and C and E are indices associated with master (mortar) nodes. In these expressions, the notations for the shape functions $N_\bullet^{(i)}$ are taken to mean the restriction of the finite element shape functions associated with either body (1) or (2) to the appropriate contact boundary. Other notations in (4)–(8) include $\boldsymbol{\lambda}_A$ for the nodal values of contact tractions at slave nodes; $\overset{*}{\boldsymbol{\varphi}}{}_B^{(1)}$ and $\overset{*}{\boldsymbol{\varphi}}{}_C^{(2)}$ for nodal values of $\overset{*}{\boldsymbol{\varphi}}{}^{(1)^h}$ and $\overset{*}{\boldsymbol{\varphi}}{}^{(2)^h}$; and $\boldsymbol{\varphi}_D^{(1)}$ and $\boldsymbol{\varphi}_E^{(2)}$ for nodal values of $\boldsymbol{\varphi}^{(1)^h}$ and $\boldsymbol{\varphi}^{(2)^h}$. The limits on the sums, n_s and n_m, are numbers of nodes on the slave (non-mortar) and master (mortar) surfaces, respectively.

Substitution of equations (4), (7) and (8) into (3) gives

$$G^{cm}(\boldsymbol{\varphi}^h, \overset{*}{\boldsymbol{\varphi}}{}^h) = -\sum_A \sum_B \sum_C \boldsymbol{\lambda}_A \cdot \left[n_{AB}^{(1)}\overset{*}{\boldsymbol{\varphi}}{}_B^{(1)} - n_{AC}^{(2)}\overset{*}{\boldsymbol{\varphi}}{}_C^{(2)}\right], \tag{9}$$

where the operators $n_{AB}^{(1)}$ and $n_{AC}^{(2)}$ are defined via:

$$n_{AB}^{(1)} = \int_{\gamma_c^{(1)^h}} N_A^{(1)} N_B^{(1)}\, d\gamma \tag{10}$$

and

$$n_{AC}^{(2)} = \int_{\gamma_c^{(1)^h}} N_A^{(1)} N_C^{(2)}\, d\gamma \tag{11}$$

Notably, it is the computation of these operators, as well as their linearizations, which constitutes most of the complexity of implementing a mortar formulation of contact. In particular, the expression for (11) involves a dependence of the surface projection of $\gamma_c^{(2)^h}$ onto $\gamma_c^{(1)^h}$ by virtue of the potentially large sliding that occurs. Detailed discussion of these implementational details will not be given here; the interested reader is referred to [4, 5] for details.

The normal and tangential portions of the contact operator are now exposed by splitting $\boldsymbol{\lambda}_A$ into normal and frictional parts:

$$\boldsymbol{\lambda}_A = \boldsymbol{\lambda}_{N_A} + \boldsymbol{\lambda}_{T_A}. \tag{12}$$

The specification of the contact treatment is completed by giving constitutive expressions for $\boldsymbol{\lambda}_{N_A}$ and $\boldsymbol{\lambda}_{T_A}$ in terms of the kinematics of the problem.

2.2 Normal contact constraints

As demonstrated previously in [4], the normal part of the contact traction may be represented as

$$\boldsymbol{\lambda}_{N_A} = -\lambda_{N_A}\boldsymbol{n}_A \text{ (no sum)} \tag{13}$$

where λ_{N_A} represents the contact pressure at node A. It is subject to Kuhn-Tucker conditions via

$$\begin{aligned} \lambda_{N_A} &\geq 0 \\ g_A &\leq 0 \\ \lambda_{N_A} g_A &= 0 \end{aligned} \tag{14}$$

where the mortar projected gap g_A at slave node A is defined as

$$\begin{aligned} g_A &= \boldsymbol{n}_A \cdot \boldsymbol{g}_A, \\ \boldsymbol{g}_A &:= \sum_B \sum_C \left[n^{(1)}_{AB}\boldsymbol{\varphi}^{(1)}_B - n^{(2)}_{AC}\boldsymbol{\varphi}^{(2)}_C \right]. \end{aligned} \tag{15}$$

Equation (15) is written in terms of a nodal normal $\boldsymbol{n}_A$, based at the *slave node*. Typically, this nodal normal is computed as some type of weighted average of the neighboring facet normals; ideas of this type and explicit expressions for the averages may be found in [4] and [5]. One may either treat equations (14) directly by using a Lagrange multiplier formulation, or consider appropriate penalty or augmented Lagrange alternatives. We have considered all three implementations in our work, although the results presented here were obtained using the penalty method.

2.3 Frictional contact conditions

The implementation of friction we consider here will be written in terms of a classical penalization of the Coulomb friction conditions, although other choices (for example, augmented Lagrangian) are certainly possible. Such a regularization is expressed via

$$\begin{aligned} \mathcal{L}_v\boldsymbol{\lambda}_T &= \epsilon_T \left[\boldsymbol{v}_T - \dot{\gamma}\frac{\boldsymbol{\lambda}_T}{\left\|\boldsymbol{\lambda}_T\right\|} \right] \\ \Phi := \left\|\boldsymbol{\lambda}_T\right\| - \mu\left\|\boldsymbol{\lambda}_N\right\| &\leq 0 \\ \dot{\gamma} &\geq 0 \\ \Phi\dot{\gamma} &= 0 \end{aligned} \tag{16}$$

where ϵ_T is the frictional penalty parameter. $\mathcal{L}_v\boldsymbol{\lambda}_T$ is the *Lie derivative* of the frictional traction, and is defined (for example) in a two dimensional problem via

$$\mathcal{L}_v\boldsymbol{\lambda}_T = \dot{\lambda}_T\boldsymbol{\tau} \tag{17}$$

where $\boldsymbol{\tau}$ is the unit tangential base vector. In (17), the time derivative contains material time derivative of components of $\boldsymbol{\lambda}_T$ only (i.e. no terms containing time derivatives of base vectors are included). It is fact that makes it a frame indifferent object.

To assure that our algorithmic representation of (16) is frame indifferent, the key additional detail needed is an algorithmic representation of the tangential relative velocity $\boldsymbol{v}_T$ within the mortar framework. In the continuum mechanical (i.e., non-algorithmic) case, the tangential component of the relative velocity is not frame indifferent when the gap g differs from zero. Frame indifference is restored in that case by adding in a dilatant portion to the tangential velocity measure (see [2]). The approach used here to assure frame indifference is similar.

To demonstrate the idea, we may look at the time continuous case first, and write the tangential component of the *mortar projected* tangential velocity at node A, which is *not* frame indifferent:

$$\boldsymbol{v}_{T_A}^{nonobj} := -\left[\sum_B n_{AB}^{(1)}\dot{\boldsymbol{\varphi}}_B^{(1)} - \sum_C n_{AC}^{(2)}\dot{\boldsymbol{\varphi}}_C^{(2)}\right]\cdot\boldsymbol{\tau}_A\otimes\boldsymbol{\tau}_A. \tag{18}$$

In (18), we have assumed two dimensions for simplicity, and written the tangent vector at node A as $\boldsymbol{\tau}_A = \boldsymbol{e}_3\times\boldsymbol{n}_A$. Objectivity is restored by including in this definition the rate of a mortar projected notion of the distance between the two bodies ($\boldsymbol{g}_A$, as is exposed in (15)), which goes to zero when perfect sliding occurs:

$$\boldsymbol{v}_{T_A} := -\left[\sum_B n_{AB}^{(1)}\dot{\boldsymbol{\varphi}}_B^{(1)} - \sum_C n_{AC}^{(2)}\dot{\boldsymbol{\varphi}}_C^{(2)} - \dot{\boldsymbol{g}}_A\right]\cdot\boldsymbol{\tau}_A\otimes\boldsymbol{\tau}_A. \tag{19}$$

One may show by direct calculation that (19) can be exactly represented via

$$\boldsymbol{v}_{T_A} = -\left[\dot{n}_{AC}^{(2)}\boldsymbol{\varphi}_C^{(2)} - \dot{n}_{AB}^{(1)}\boldsymbol{\varphi}_B^{(1)}\right]\cdot\boldsymbol{\tau}_A\otimes\boldsymbol{\tau}_A \tag{20}$$

where $\dot{n}_{AC}^{(2)}$ and $\dot{n}_{AB}^{(1)}$ are time derivatives of the mortar integrals. It is the tangential velocity in (20) that we will numerically approximate in our numerical formulation.

In this paper, a trial state-return map strategy is employed to determine the Coulomb frictional traction, with the constitutive law being obtained by application of a backward Euler strategy to the equations obtained by substitution of (20) into (16). As in [2], we first compute a trial state, assuming no slip during the increment:

$$\lambda_{T_{A_{n+1}}}^{trial} = \lambda_{T_{A_n}} - \epsilon_T\boldsymbol{\tau}_A\cdot\left[\sum_C\left(n_{AC_{n+1}}^{(2)} - n_{AC_n}^{(2)}\right)\boldsymbol{\varphi}_C^{(2)} - \sum_B\left(n_{AB_{n+1}}^{(1)} - n_{AB_n}^{(1)}\right)\boldsymbol{\varphi}_B^{(1)}\right] \tag{21}$$

and we define a trial value for the slip function via

$$\Phi_{n+1}^{trial} = \left\|\boldsymbol{\lambda}_T^{trial}\right\| - \mu\left\|\boldsymbol{\lambda}_N\right\|. \tag{22}$$

Then the return map used to define the final frictional traction is given as:

$$\boldsymbol{\lambda}_{T_{A_{n+1}}} = \begin{cases} \boldsymbol{\lambda}^{trial}_{T_{A_{n+1}}} = \lambda^{trial}_{T_{A_{n+1}}} \boldsymbol{\tau}_A & \text{if } \left(\Phi^{trial}_{n+1}\right) \leq 0, \text{ stick}, \\ \mu \left\| \boldsymbol{\lambda}_{N_A} \right\| \boldsymbol{\tau}_A & \text{otherwise, slip} \end{cases} . \tag{23}$$

In these expressions, the subscript $n+1$ means a state associated with the current iteration of the $n+1$st load (or time) step, and n is to be associated with the n-th converged load step.

3 NUMERICAL EXAMPLE

To provide a brief demonstration of the effectiveness of the approach advocated, we consider a two dimensional example where a block is pressed into an elastic slab and then slid over the surface. The material for both the block and the slab are assumed to be Neohookean hyperelastic. The bulk and shear modulus of the slab are $K = 63.84 \times 10^7$ and $G = 26.12 \times 10^7$, while the block is taken to be ten times stiffer than the slab. The geometric properties are shown in Figure 1. The bottom surface of the slab is fixed. Through displacement control, the top of the block travels $p = 1.8$ in the vertical direction from time $0 - 1$ and then $q = 10$ in the horizontal direction from time $1 - 2$. The finite element meshes are shown in Figure 2. The deformations at $t = 1.0$, $t = 1.5$ and $t = 2.0$ are shown in Figure 3. Coulomb friction is considered in this problem, with the coefficient of friction being $\mu = 0.3$.

The reaction loads computed on the top of the block are shown in Figure 4. It can be noticed that at time between 1.0 and 1.1 we have to push harder because of the resistance caused by the contact of the side surface with the slab. Interestingly, the more traditional node-to-segment contact formulation fails at time 0.66. Particularly notable is the fact that despite the large deformations featured by this example, the load-displacement response is relatively smooth and the performance of the solution procedure is highly robust. In large part, this occurs because of the non-local character of the contact discretization procedure, which acts to smooth the discontinuities in the contact kinematics resulting from the faceted finite element discretization of the contact surface.

4 CONCLUSIONS

A method for incorporating friction into mortar-finite element descriptions of large deformation contact mechanics has been presented. As has been demonstrated, the framework allows for frame indifferent description of frictional laws, and produces highly robust contact algorithms even in the context of large deformations and large amounts of relative sliding.

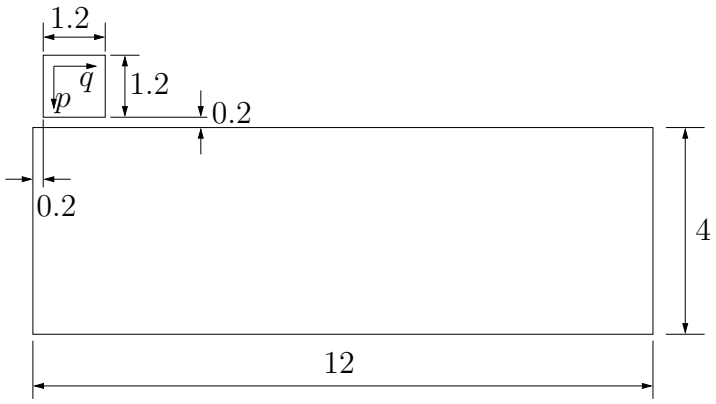

Figure 1: The initial configuration of the ironing problem.

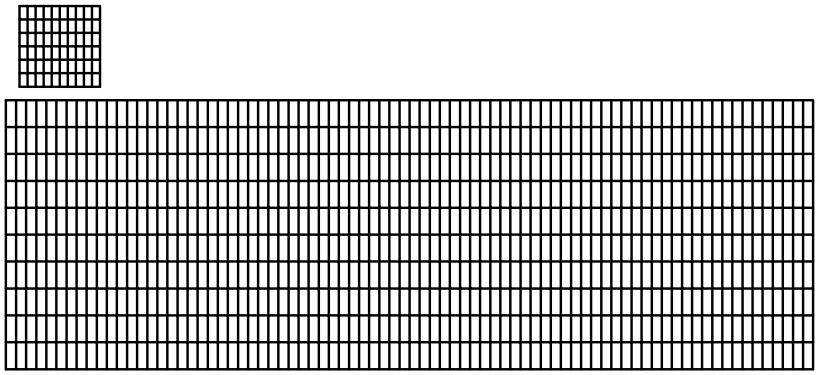

Figure 2: The finite element mesh of the ironing problem.

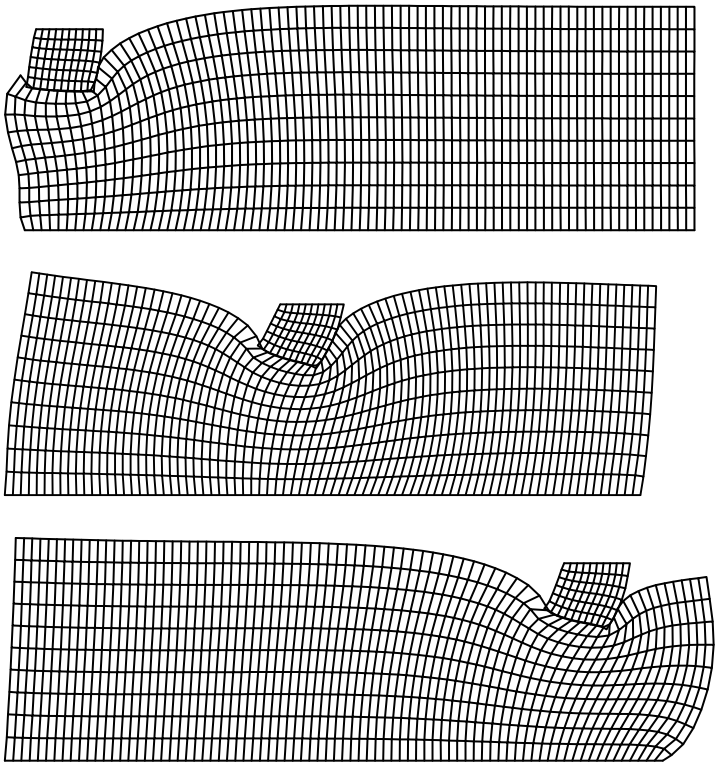

Figure 3: Deformed configurations for the ironing problem at $t = 1.0$, $t = 2.0$ and $t = 3.0$.

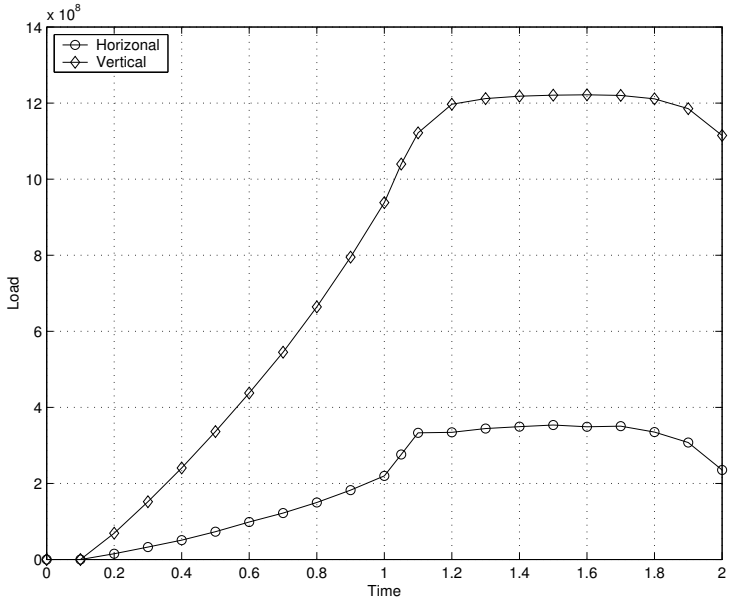

Figure 4: Computed load vs. time (load parameter) curves; ironing problem.

REFERENCES

[1] P. Hild. Numerical Implementation of Two Nonconforming Finite Element Methods for Unilateral Contact. *Computer Methods in Applied Mechanics and Engineering*, **184**, 99–123, 2000.

[2] T.A. Laursen. *Computational Contact and Impact Mechanics*. Springer, Berlin, 2002.

[3] T.W. McDevitt and T.A. Laursen. A Mortar-Finite Element Formulation for Frictional Contact Problems. *International Journal for Numerical Methods in Engineering*, **48**, 1525–1547, 2000.

[4] M.A. Puso and T.A. Laursen. A Mortar Segment-to-Segment Contact Method for Large Deformation Solid Mechanics. *Computer Methods in Applied Mechanics and Engineering*, **193**, 601–629, 2004.

[5] B. Yang, T.A. Laursen and X. Meng. Two Dimensional Mortar Contact Methods for Large Deformation Frictional Sliding. *International Journal for Numerical Methods in Engineering*, submitted, 2004.